Supplementary Information

Garlic-derived exosome-like nanovesicles alleviate dextran sulphate sodium-induced colitis in mice via TLR4/MyD88/NF-κB pathway and gut microbiota modulation

Zhenzhu Zhu*[a], Liuyue Liao[a], Mingwei Gao[a], Qin Liu[a]

[a] College of Food Science and Engineering, Nanjing University of Finance and Economics, Collaborative Innovation Center for Modern Grain Circulation and Safety, Nanjing 210023, People's Republic of China

Supplemental materials and methods

Analysis of purity, size, and zeta potential of GENs

The size and number of GENs (12.6 mg/mL) were measured by nanoparticle tracking analysis (NTA) on the Nanosight NS300 (Malvern Instruments, Malvern, UK). The hydrodynamic size and polydispersity index (PDI) of GENs were assessed by dynamic light scattering (DLS) on the Nano ZS (Malvern Instruments, Malvern, UK). Zeta potential of GENs was determined by electrophoretic light scattering on a Zetasizer Nano ZS (Malvern Instruments, Malvern, UK).

Cellular uptake and cell viability assays

Caco-2 cells were cultured in Dulbecco's modified eagle medium (DMEM, Gibco, Grand Island, NY, USA), supplemented with penicillin-streptomycin solution (Beijing Solarbio Science & Technology Co., Ltd., Beijing, China) and fetal bovine serum (20%, Gibco, Grand Island, NY, USA) at 37 ℃ in a humidified atmosphere containing 5%

CO_2. Caco-2 cells were seeded in 6-well plates for 24 h. Before assay, GENs were labeled with PKH67 (Beijing Baiaolaibo Technology Co., Ltd, Beijing, China) for 15 min at 37 ℃ and for 15 min at 4 ℃. For uptake assay, Caco-2 cells seeded in φ15mm glass bottom dish (2×10^5 cells/plate) were incubated with PKH67-labeled GENs (20 μg/mL) for 2, 4, and 6 h, respectively. Afterward, the cells were washed with PBS, cellular nuclei were stained with Hoechst 33342. Finally, cells were imaged using Eclipse C1 fluorescence microscopy (Nikon, Japan). The excitation wavelengths of PKH67 and Hoechst 33342 (Shanghai Byotime Biotechnology Co., Ltd., Shanghai, China) were set at 490 nm and 350 nm, respectively.

For cell viability assay, Caco-2 cells were seeded in 96-well plates at a density of 5×10^4 cells/well for 48 h. Then, Caco-2 cells were treated with GENs (1, 10, 20, 40, 80 μg/mL) with or without LPS (1 μg/mL) stimulation for 24 h. 3-(4,5-dimethythiazol-2-yl)-2,5-diphenyl tetrazolium bromide (MTT, Shanghai Byotime Biotechnology Co., Ltd., Shanghai, China) (20 μL) was added and incubated for 4 h. Next, dimethylsulfoxide (DMSO, 150 μL) was added to resolve the formazan. The optical density (OD) value at 490 nm was measured by using an ELISA microplate reader (SpectraMax M2, USA) after shaking for 15 min. The cell viability was calculated by the formula: cell viability rate (%) = $(OD_{490,\ drug} - OD_{490,\ blank})/(OD_{490,\ control} - OD_{490,\ blank})\times100\%$.

Lucifer yellow (LY) assay

Caco-2 cells were treated with GENs (0, 1, 5, 10 μg/mL) and LPS (1 μg/mL) for 24 h. LY was added to the apical chambers, and the mixture was incubated for 2 h. The culture media from the basolateral chambers were then collected, and the fluorescence intensity of samples was measured by using a multifunctional microplate reader. The excitation and emission wavelengths of LY were set at 428 nm and 540 nm,

respectively. Apparent permeability coefficient (Papp) in the Caco-2 monolayer cells was calculated as previously reported.[1]

Supplemental Figures and Tables

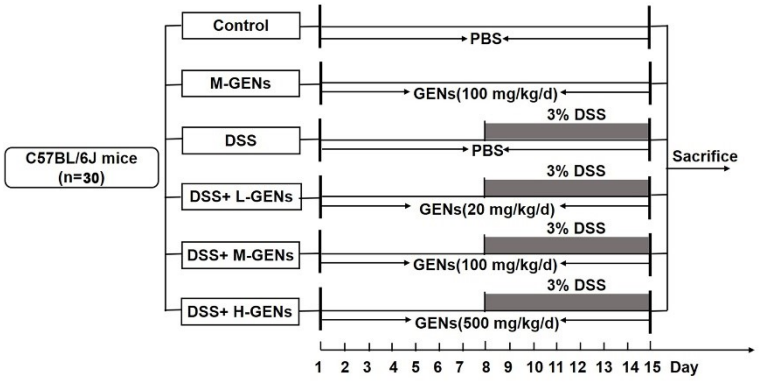

Fig. S1 The establishment of DSS-induced mice colitis model and the administration strategy of GENs (20, 100, 500 mg/kg).

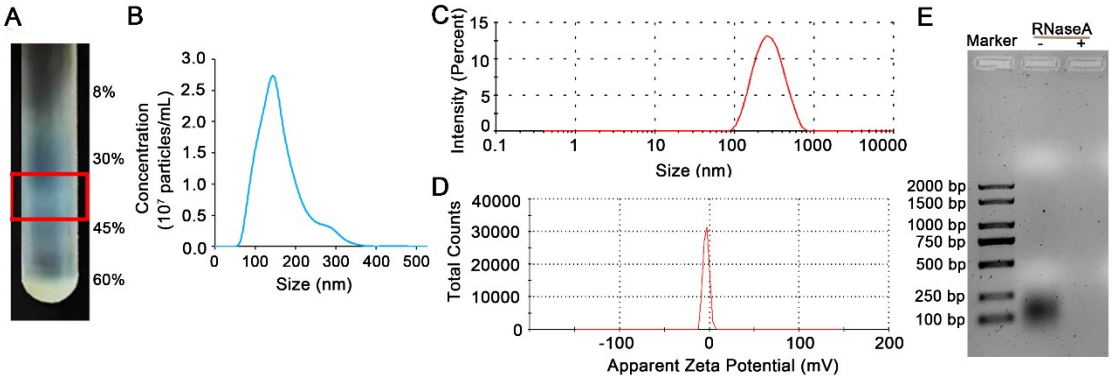

Fig. S2 Characterization of GENs. (A) Suspension of GENs in the sucrose gradients (30-45%) after ultracentrifugation. (B) The size distribution, (C) hydration diameter distribution, and (D) zeta potential of GENs. (E) Agarose gel of total RNAs.

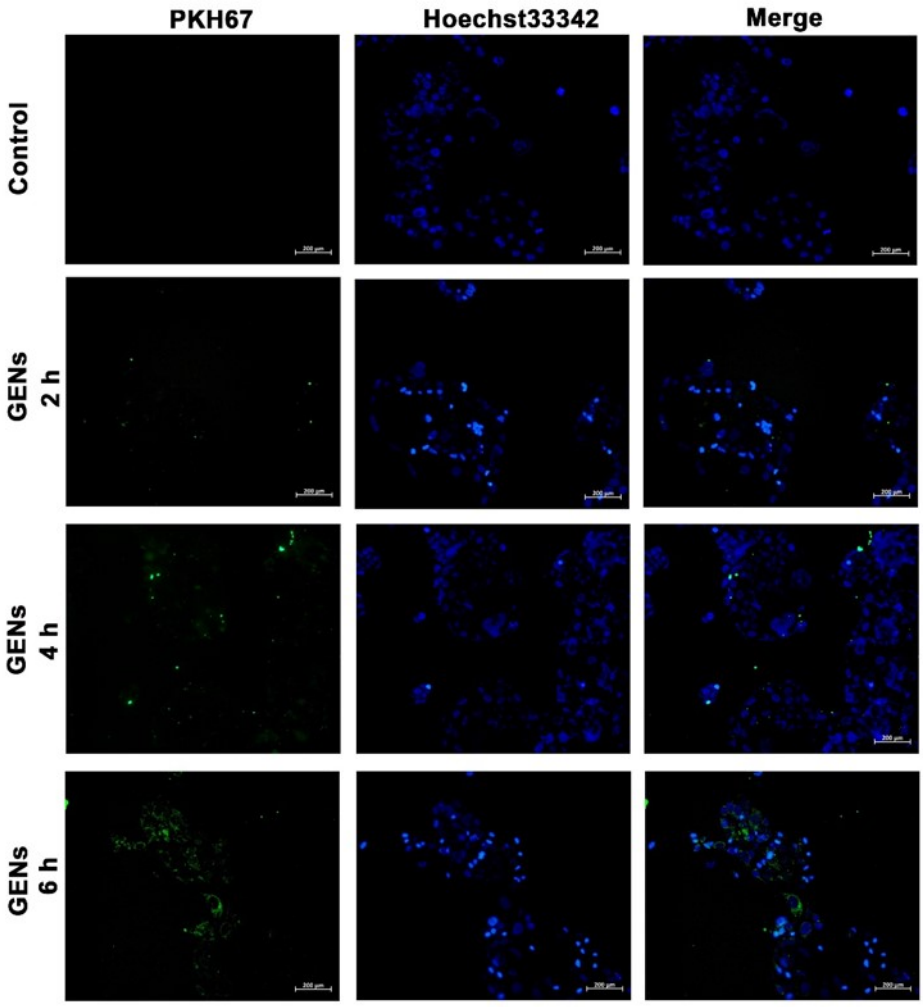

Fig. S3 Cellular uptake of GENs (20 μg/mL) labeled by PKH67 (green) after co-incubating with Caco-2 cells for 2, 4, 6 h at 37 °C. The nuclei were labeled by Hoechst 33342 (blue), the scale bar was 200 μm.

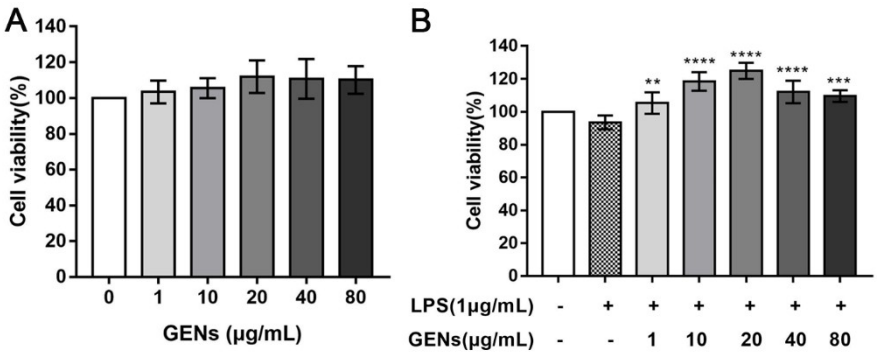

Fig. S4 The cell viability of Caco-2 cells after GENs treatment with or without LPS (1 μg/mL) stimulation. $^{**}p < 0.01$, $^{***}p < 0.001$, $^{****}p < 0.0001$, GENs group *vs* LPS group.

Fig. S5 Survival rate of C57BL/6J mice in the control, DSS, L-GENs, M-GENs, and H-GENs groups.

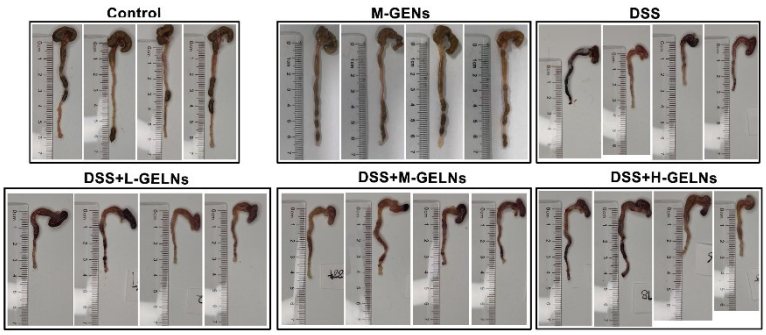

Fig. S6 Photos of colon tissues in the normal mice (control), M-GENs treated C57BL/6J mice at the 15th day, DSS treated C57BL/6J mice, DSS + L-GENs treated, DSS + M-GENs treated and DSS + H-GENs treated mice at the 15th day. The length of colon tissue was measured by a rule.

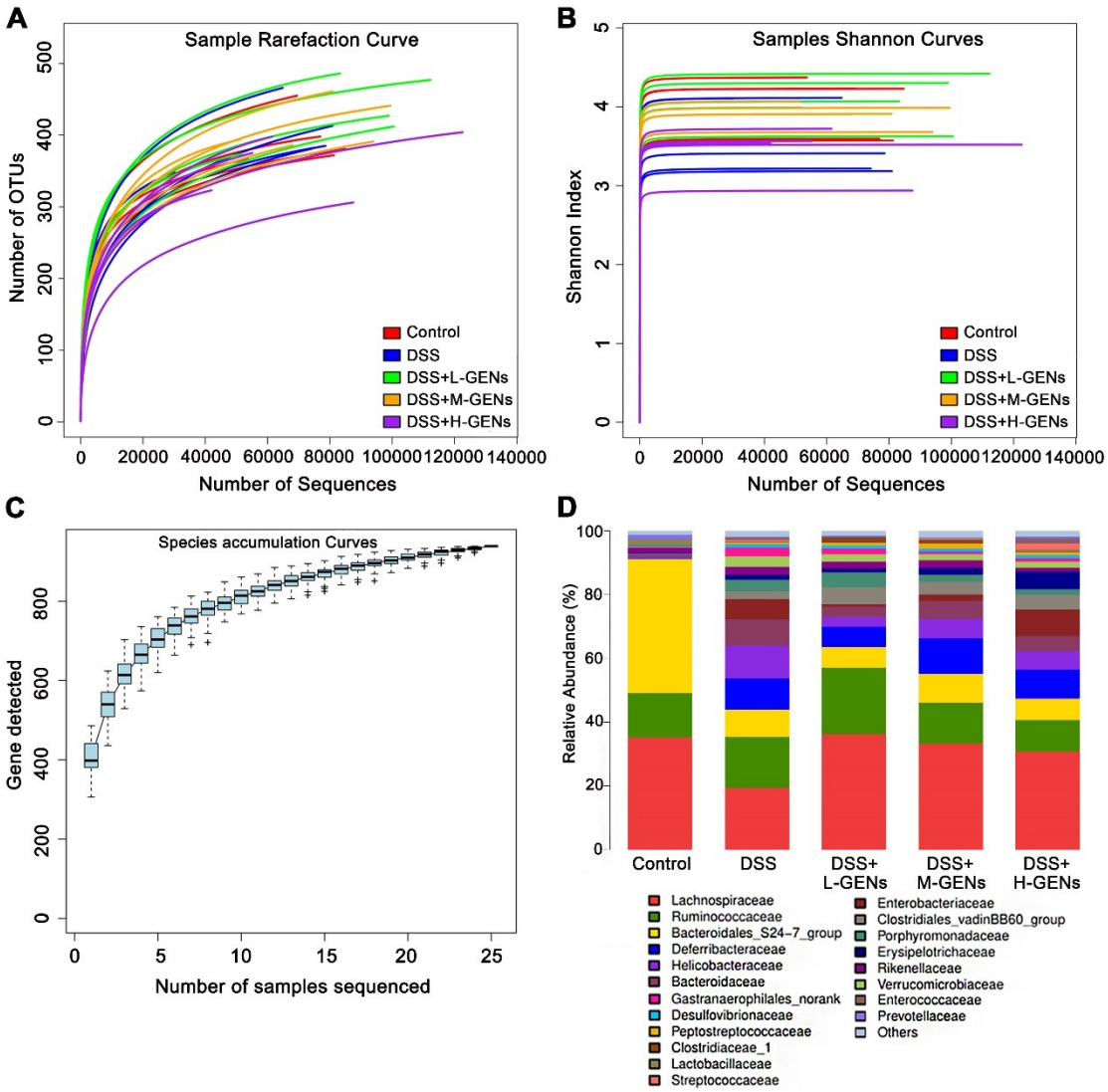

Fig. S7 The rarefaction curve (A), Shannon curve (B) and species accumulation curve (C) of cecal contents, the relative quantitation of domain bacteria at the family level (D).

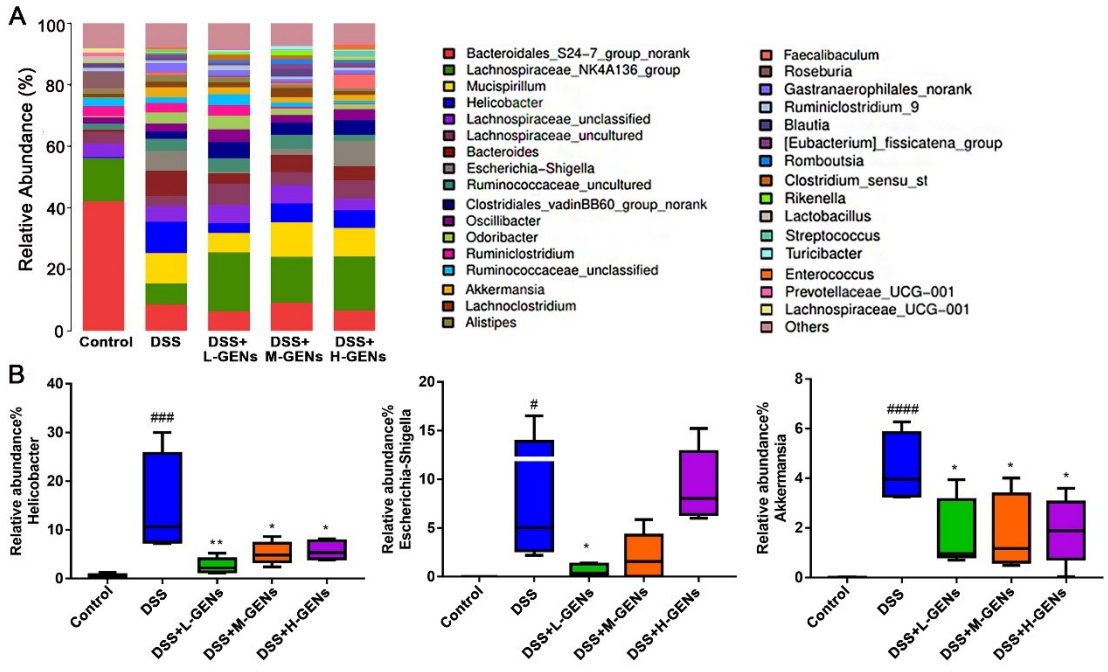

87

88 **Fig. S8** (A) Distribution of gut microbiota at the genus level. (B) The relative

89 abundance of *Helicobacter*, *Escherichia-Shigella* and *Akkermansia.* $^{\#}p<0.05$,

90 $^{\#\#\#}p<0.001$, $^{\#\#\#\#}p<0.0001$, DSS group *vs* control; $^{*}p<0.05$, $^{**}p<0.01$, DSS + GENs group

91 *vs* DSS group.

92

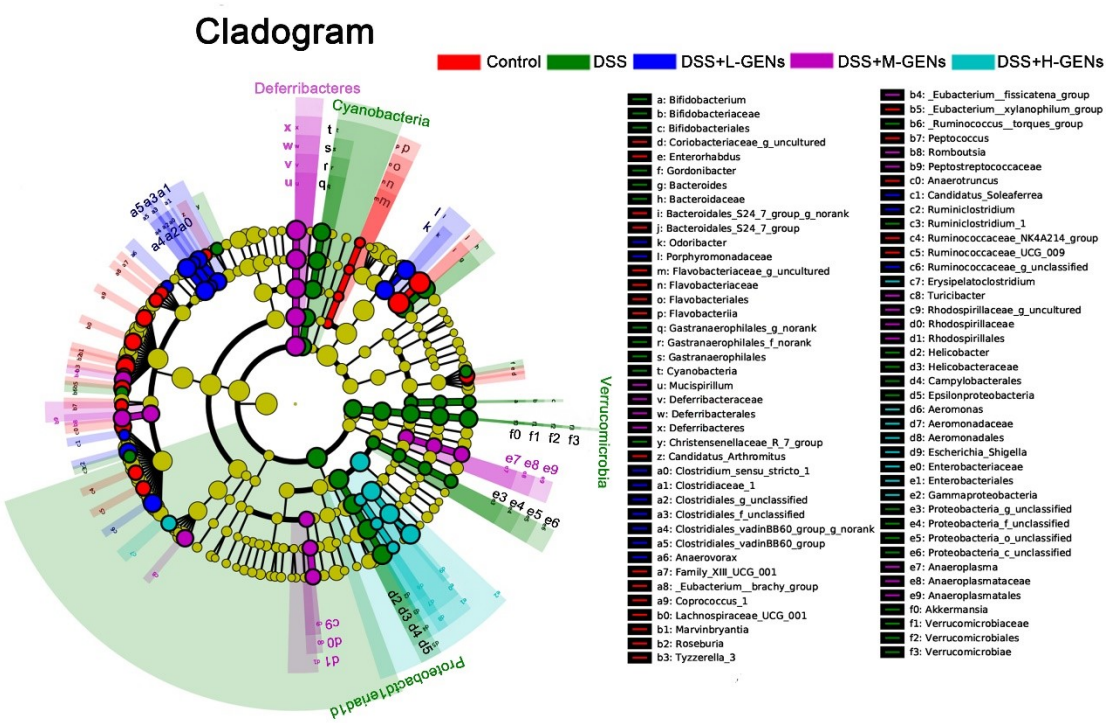

Fig. S9 Taxonomic cladogram of the main different microbiota by linear discriminant analysis effect size (LEfSe). Control group (red), DSS group (green blue), DSS + L-GENs group (blue), DSS + M-GENs group (purple) and DSS + H-GENs group (cyan). Yellow color represented that the taxa having no significant difference.

Table S1. Disease activity index (DAI)[2]

Score	Weight loss (%)	Bloody stools	Stool consistency
0	None	Normal	None
1	1-5	-	-
2	5-10	Soft and shaped	Slight bleeding
3	10-15	-	-
4	＞15	Diarrhea	Gross bleeding

101 **Table S2.** Histopathology grading system for colonic sections[3]

Feature graded	Grade	Description
inflammation	0	normal
	1	minimal infiltration of lamina propria, focal to multifocal
	2	mild infiltration of lamina propria, multifocal, mild gland separation
	3	moderate to mixed infiltration, multifocal with minimal edema
	4	marked mixed infiltration into submucosa and lamina propria with extensive areas of gland separation, enlarged Peyer's patches, edema
epithelium	0	normal
	1	minimal: focal mucosal hyperplasia
	2	mild: multifocal tufting of rafts of epithelial cells with increased numbers of goblet cells
	3	moderate: multifocal to locally extensive epithelial attenuation or erosion with goblet cell hyperplasia
	4	marked: locally extensive to subtotal erosion or ulceration
glands	0	normal
	1	minimal: rare gland dilatation
	2	mild: multifocal gland dilatation
	3	moderate: multifocal gland dilatation with abscessation and occasional loss of glands
depth of lesion	0	none
	1	mucosa
	2	mucosa and submucosa
	3	transmural
extent of section affected	0	none
	1	minimal: <10%
	2	mild: 10−25%
	3	moderate: 26−50%
	4	marked: >50%

102

Table S3. Primer sequences used for RT-qPCR[4]

Gene	Primer sequence (5'-3')
β-actin-Forward	TCAGCAAGCAGGAGTACGATG
β-actin-Reverse	AACGCAGCTCAGTAACAGTCC
TLR4-Forward	ACTTCCATCCAGTTGCCTTCTTGG
TLR4-Reverse	TTAAGCCTCCGACTTGTGAAGTGG
MyD88-Forward	TCTCGGACTCCTGGTTCTGCTG
MyD88-Reverse	TCTCGGACTCCTGGTTCTGCTG

Table S4. Basic parameters of garlic-derived exosome-like nanovesicles

Parameters (unit)	Value	Method
Yield (p/mL)	$(2.86 \pm 0.15) \times 10^9$	NTA
Particle-to-protein ratio (p/μg)	$(8.17 \pm 0.43) \times 10^7$	-
Particle size/nm	160.20 ± 3.50	NTA
Hydration diameter/nm	229.33 ± 3.26	DLS
Zeta/mV	-10.07 ± 0.78	-
PDI	0.21 ± 0.00	-

Table S5. The class and percentage of lipids in garlic-derived exosome-like nanovesicles by the lipidomic analysis.

No.	Class	Abbreviation	Percentage/%
1	phosphatidylcholine	PC	27.6780
2	acyl hexosyl sitosterol ester	AcHexSiE	16.2776
3	sphingosine	SPH	15.2774
4	triglyceride	TG	10.3309
5	ceramide	Cer	6.5079
6	phosphatidylethanolamine	PE	5.9138
7	wax ester	WE	4.1815
8	diacylglycerol	DG	3.9531
9	phosphatidylethanol	PEt	2.5091
10	acyl hexosyl campesterol ester	AcHexCmE	2.2218
11	acyl hexosyl stigmasterol ester	AcHexStE	1.3953
12	Hexosylceramide	Hex1Cer	0.7897
13	acyl hexosyl zymosterol ester	AcHexZyE	0.4791
14	monoglyceride	MG	0.4393
15	phospholipids alcohol	PA	0.4190
16	acyl hexosyl cholesterol ester	AcHexChE	0.2632
17	lysophosphatidylcholine	LPC	0.2521
18	phosphatidylglycerol	PG	0.2481
19	(O-acyl)-1-hydroxy fatty acid	OAHFA	0.2354
20	monogalactosyldiacylglycerol	MGDG	0.1686
21	phosphatidylinositol	PI	0.1355
22	phosphatidylserine	PS	0.1070
23	lysophosphatidylethanolamine	LPE	0.0762
24	digalactosyldiacylglycerol	DGDG	0.0699
25	N-Acylethanolamine	AEA	0.0387
26	lysobisphosphatidic acid	LBPA	0.0319

Table S6. The affiliation of proteins in garlic-derived exosome-like nanovesicles by the proteomic analysis.

No.	Identified Proteins	Protein Existence[a]	Accession Number	Molecular Weight
1	Acetolactate synthase	2	A0A3S7QFS2_ALLFI	71 KDa
2	Adenosylhomocysteinase (Fragment)	2	Q9SDP1_ALLCE	34 KDa
3	Aldehyde dehydrogenase (Fragment)	2	Q8RVW3_ALLCE	30 KDa
4	Alliinase (Fragment)	3	Q9SW86_ALLSA	33 KDa
5	Alliinase	2	A0A3G2I868_ALLPO	55 KDa
6	Aquaporin 1	2	Q9M4T0_ALLCE	31 KDa
7	Aquaporin 2	2	Q9M4S9_ALLCE	31 KDa
8	Aquaporin plasma in insic protein 1	2	A0A0D4CZJ2_ALLSA	31 KDa
9	Aquaporin plasma in insic protein 2	2	A0A0D4CZX5_ALLSA	31 KDa
10	Aquaporin plasma in insic protein 3	2	A0A0D4CYY1_ALLSA	31 KDa
11	ATP synthase subunit alpha (Fragment)	3	A1XIV0_ALLCE	46 KDa
12	ATP synthase subunit beta chloroplastic	3	A0A6B9VW32_9ASPA	54 KDa
13	ATP-dependent Clp protease proteolytic subunit	3	A0A6B9VXS4_9ASPA	23 KDa
14	Beta-actin	2	A0A345F2T1_ALLCE	42 KDa
15	Bifunctional 6(G)-fructosyltransferase/2 1-fructan:2 1-fructan 1-fructosyltransferase	1	P92916|GFT_ALLCE	69 KDa
16	Cell division cycle protein 48 homolog	2	G5EIQ1_ALLCE	90 KDa
17	Cysteine synthase	2	Q9MAZ2_ALLTU	34 KDa
18	Cysteine synthase	2	Q3L195_ALLSA	36 KDa
19	Cytochrome oxiIIdase subunitII (Fragment)	4	A0A059XHT2_9ASPA	10 KDa
20	Defensin 3	2	A0A7D5T120_ALLSA	8 KDa
21	Defensin 5	2	A0A7D5NM87_ALLCE	9 KDa

No.	Identified Proteins	Protein Existence[a]	Accession Number	Molecular Weight
22	Defensin 5	4	A0A7D5NJX8_ALLCE	9 KDa
23	DnaJ protein homolog	2	P42824|DNJH2_ALLPO	47 KDa
24	Farnesyl diphosphate synthase	2	F6KUJ4_ALLSA	40 KDa
25	Flavonoid glucosyl- transferase	2	Q7XJ49_ALLCE	53 KDa
26	Glutamate--cysteine ligase	2	Q8W1X9_ALLCE	56 KDa
27	Glutathione transferase	2	A4PIV6_ALLCE	24 KDa
28	Glutathione-S-transferase	2	A0A5J6YHL6_ALLSA	26 KDa
29	Glyceraldehyde-3-phosphate dehydrogenase (Fragment)	3	D2KCJ8_ALLSC	19 KDa
30	Glyceraldehyde-3-phosphate dehydrogenase (Fragment)	3	A0A076V7J0_ALLCE	21 KDa
31	Glyceraldehyde-3-phosphate dehydrogenase GAPC2 (Fragment)	3	A0A2S1IZX9_ALLPO	21 KDa
32	Glyoxalase	2	F2ZC02_ALLCE	33 KDa
33	GTP-Binding Nuclear Protein Ran-2	2	A9X4K0_ALLSA	25 KDa
34	Heat shock protein 70 homologue (Fragment)	2	Q43372_ALLCE	15 KDa
35	Heat shock protein 70	2	H2CLX1_ALLSA	40 KDa
36	Histone H4 (Fragment)	2	Q38686_ALLCE	7 KDa
37	I lectin (Fragment)	1	Q38789_ALLSA	33 KDa
38	II lectin (Fragment)	1	Q38783_ALLSA	17 KDa
39	Lectin (Fragment)	4	K4P0T2_ALLSA	32 KDa
40	Lactoylglutathione lyase	2	F5HSC6_ALLCE	21 KDa
41	Late embryogenesis abundant protein lea14-a	2	H2CLX2_ALLSA	17 KDa
42	Lipoxygenase	2	A0A1J0I8W4_ALLCE	99 KDa
43	Molecular chaperone DjA2	2	Q0GLI7_ALLPO	47 KDa
44	Peptidylprolyl cis-trans isomerase	2	P34887|CYPH_ALLCE	16 KDa
45	Peroxidase ATP17a-like protein	2	H2CLX6_ALLSA	21 KDa
46	Phospholipase D alpha (Fragment)	2	C7SAX4_ALLPO	21 KDa
47	Proteasome subunit alpha-3 (Fragment)	2	Q6U835_ALLSA	16 KDa
48	Protein TIC 214	3	A0A4Y5X071_9ASPA	210 KDa

No.	Identified Proteins	Protein Existence[a]	Accession Number	Molecular Weight
49	Putative cold-regulated protein	2	H2CLX4_ALLSA	26 KDa
50	Putative progesterone 5-beta-reductase	2	A0A0M4BW04_ALLUR	44 KDa
51	Sucrose:sucrose 1-fructosyl transferase 1-SST	2	A0A125SXW5_ALLCE	70 KDa
52	Sucrose:sucrose 1-fructosyl transferase 1-SST	2	Q8LPM7_ALLSA	70 KDa
53	Sucrose-phosphate synthase (Fragment)	2	A8IK45_ALLCE	114 KDa
54	Superoxide dismutase (Fragment)	2	D2Y1A6_ALLSA	15 KDa
55	Tau glutathione S-transferase	2	F2ZC01_ALLCE	26 KDa
56	trypsin inhibitor	2	Q8RVY7_ALLCE	11 KDa
57	Tubulin beta chain	2	A0A345F2T2_ALLCE	50 KDa
58	Uncharacterized protein	2	H2CLX8_ALLSA	22 KDa
59	Unspecific 9/13 divinyl ether synthase	2	Q2WE96_ALLSA	53 KDa
60	Vacuolar H+-ATPase catalytic subunit (Fragment)	2	Q9SDP0_ALLCE	20 KDa
61	Vacuolar H+-ATPase catalytic subunit (Fragment)	2	Q9SDM0_ALLCE	22 KDa

[a] Protein Existence. 1. Experimental evidence at protein level; 2. Experimental evidence at tran level;3. Protein inferred from homology; 4. Protein predicted; 5. Protein uncertain. The raw file was submitted to the established database by using the PEAKS Studio 8.5 software, and the whole Allium of UniProt database was used for comparative search (https://www.uniprot.org/taxonomy/4678). The filter parameters of result: Peptide FDR≥1%, unique peptide≥1.

Table S7. The name, sequence and reads count of miRNAs in garlic-derived exosome-like nanovesicles by microRNA sequencing[a].

No.	Name	Sequence	Reads Count
1	han-miR3630-5p	GCAAGUGAUGAAGAACCA	16717
2	aof-miR166a	UCUCGGACCAGGCUUCAUUCC	971
3	ata-miR166c-3p	UCGGACCAGGCUUCAUUCCUU	748
4	sly-miR166c-3p	UCGGACCAGGCUUCAUUCCUC	684
5	ppt-miR894	UUCACGUCGGGUUCACCA	451
6	aof-miR159	UUUGGAUUGAAGGGAGCUCU	981
7	aof-miR396a	UUCCACGGCUUUCUUGAACUG	385
8	aof-miR166d	UCGGACCAGGCUUCAUUCCCC	165
9	aof-miR394	UUGGCAUUCUGUCCACCUCC	85
10	aof-miR396b	UUCCACAGCUUUCUUGAACUG	75
11	sly-miR168a-3p	CCUGCCUUGCAUCAACUGAAU	75
12	aof-miR390	AAGCUCAGGAGGGAUAGCGCC	40
13	aof-miR167b	UGAAGCUGCCAGCAUGAUCUGA	37
14	aof-miR166b	UCUCGGACCAGGCUUCAUUC	69
15	gma-miR482d-3p	UCUUCCCUACACCUCCCAUACC	31
16	eun-miR482a-3p	UCUUGCCAAUACCACCCAUGCC	28
17	lja-miR171c	UGAGCCGAAUCAAUAUCACUU	26
18	aof-miR536	UCGUGCCACGCUGUGUGCGUC	14
19	mes-miR156k	UUGACAGAAGAGAGAGAGCAC	11
20	aof-miR535	UGACAACGAGAGAGAGCACGC	12
21	cas-miR394	UUUGGCAUUCUGUCCACCUCC	9
22	aof-miR319a	UUGGACUGAAGGGAGCUCCCU	22
23	tae-miR9777	AGCAACUUAUCUGAGCAC	9
24	cas-miR159b-3p	UUUGGAUUGAAGGGAGCUCUU	7
25	gso-miR1510a	UGUUGUUUUACCUAUUCCACC	12
26	aof-miR827	UUAGAUGGCCAUCAACAAACA	7

No.	Name	Sequence	Reads Count
27	gso-miR3522b	UGAGACCAAAUGAGCAGCUGA	6
28	lja-miR1511-3p	AACCAGGCUCUGAUACCAUGA	7
29	aof-miR164	UGGAGAAGCAGGGCACGUGCA	8
30	vun-miR2118	UUGCCGAUUCCACCCAUUCCU	7
31	bra-miR158-3p	UUUCCAAAUGUAGACAAAGCA	8
32	gma-miR1510b-5p	AGGGAUAGGUAAAACAACU	8
33	aof-miR167c	UGAAGCUGCCAGCAUGAUCU	8
34	csi-miR166f-3p	UCGGACCAGGCUUCAUUCCCU	5
35	bdi-miR7717c-3p	GUUAGUGAUGAGAAAUAG	5
36	gso-miR1507b	UCUCAUUCCAUACAUCGUCUGA	6
37	csi-miR1515b-5p	UCAUUUUUGCGUGCAGUGAUCC	5
38	pab-miR11407a	AAACUCUGACGGCGCAAC	5
39	aof-miR319b	UUUGGACUGAAGGGAGCU	12
40	gma-miR2109-3p	GGAGGCGUAGAUACUCACACC	4
41	gma-miR1513b	UGAGAGAAAGCCAUGACUUAC	4
42	pab-miR156w	UUGACAGAAGAUAGAGGGCAC	5
43	cas-miR166a	GGAAUGUUGUCUGGCUCGU	8
44	cas-miR159a	UUUGGAUUGAAGGGAGCUCC	4
45	aqc-miR159	UUUGGACUGAAGGGAGCUCU	5
46	aof-miR168a	UUCGCUUGGUGCAGGUCGGGA	7
47	csi-miR393b-5p	UUCCAAAGGGAUCGCAUUGAUC	3
48	aof-miR156a	UGACAGAAGAGAGUGAGCAC	5
49	pab-miR396t	UUCCACGGCUUUCUUGAACUU	3
50	aof-miR160c	UGCCUGGCUCCCUGUAUGCCA	4
51	vca-miR167b-3p	AGAUCAUGUUGCAGUUUCAUC	4
52	gma-miR4412-5p	UGUUGCGGGUAUCUUUGCCUC	4
53	eun-miR482b-3p	UUUCCUAUUCCUCCCAUUCCA	3
54	aof-miR171c	UUGAGCCGCGUCAAUAUCUC	7

No.	Name	Sequence	Reads Count
55	osa-miR444c.1	UGUCUCAAGCUUGCUGCCU	4
56	gma-miR5372	UUGUUCGAUAAAACUGUUGUG	3
57	osa-miR5807	GGGCUGGGGUUAUGUGGC	3
58	cas-miR858	UUCAUUGUCUGUUCGACCU	2
59	bra-miR168a-3p	CCCGCCUUGUGUCAAGUGAAU	2
60	aly-miR4226	ACAACAUGAUCGAGCAAU	2
61	pab-miR396a-5p	UUCCACAGCUUUCUUGAACUA	2
62	bdi-miR166e-3p	CUCGGACCAGGCUUCAUUCCC	2
63	eun-miR482c-5p	GAGAUUCGAGCUACCGGAAGUCGUG	2
64	gso-miR2109	UGCGAGUGUCUUCGCCUCUGA	3
65	stu-miR1886g-5p	GAUGGACAAGGUUUGGACA	2
66	csi-miR396f-5p	UUCCACAGCUUUCUUGAACUU	2
67	gso-miR1509a	UUAAUCAAGGAAAUCACGGUCG	1
68	gma-miR1510a-3p	UGUUGUUUUACCUAUUCCACCC	2
69	gma-miR319q	UGGACUGAAGGGAGCUCCUUC	1
70	lus-miR159b	UUUGGAUUGAAGGGAGCUCUC	2
71	pvu-miR159a.2	CUUCCAUAUCUGGGGAGCU	4
72	sly-miR319c-3p	UUGGACUGAAGGGAGCUCCUU	2
73	mtr-miR166b	UCGGACCAGGCUUCAUUCCUA	1
74	ppt-miR166m	UCGGACCAGGCAUCAUUCCUU	1
75	ptc-miR166p	UCGGACCAGGCUCCAUUCCUC	1
76	cpa-miR167c	UGAAGCUGCCAGCAUGAUCUU	1
77	bra-miR168c-5p	GCGCUUGGUGCAGGUCGGGAC	2
78	bdi-miR169d	UAGCCAAGAAUGACUUGCCUC	1
79	lus-miR171j	UGAUUGAGCCGCGUCAAUAUC	2
80	ppe-miR171d-5p	CGUGAUAUUGGUUCGGUU	2
81	zma-miR2275a-5p	GUUGGAGCAAAGCAAACC	1
82	ppt-miR390c-3p	CGCUGUCCGAUUUGAGCA	1

No.	Name	Sequence	Reads Count
83	stu-miR399i-3p	UGCCAAAGGAGAGUUGCCCUA	1
84	gra-miR482	CUUCCAAUUCCUCCCAUU	1
85	gma-miR5380b	GAAAAUGAAGAUGGAGGA	1
86	sbi-miR5564a	GGAAGAAUUUGUCGAACA	2
87	gma-miR5670b	CACAUCAUACCAUAUUUGCUUC	1
88	nta-miR6025d	GAACAAUUGAAUAACUCUA	1
89	bdi-miR827-5p	GUUUUGUUGGUUGCAUCU	1
90	aof-miR12149	GCUUCUUUGUCAUACUUCU	1
91	aof-miR156b	UUGACAGAAGAUAGAGAGCAC	1
92	aof-miR166c	UCGGACCAGGCUUCAUCCCCC	1
93	aof-miR168b	UCGCUUGGUGCAGGUCGGG	2
94	aof-miR171b	UUGAGCCGCGCCAAUAUCACG	2
95	aof-miR172	AGAAUCUUGAUGAUGCUGCAUU	2
96	ath-miR8175	UCCCUGGCAACGGCGCCA	1
97	bdi-miR5057	AUUUCAAAUCGUUUGACA	1
98	bdi-miR845	GCUCUGAUACCAAUUGUU	1
99	bra-miR5721	AAAAAAGGAGUGAGAAUGGA	1
100	cas-miR166f-3p	UCGGACCAGGCUUCAUUCCCCU	1
101	cme-miR854	UGAGGAUGAGGAGGAGGA	2
102	csi-miR159c-3p	CUUGGACUGAAUGGAGCUCCC	1
103	csi-miR169r-5p	CAGCCAAGGAUGACUUGCC	2
104	csi-miR171f-5p	UAUUGGCCUGGUUCACUCAGA	1
105	csi-miR395c-3p	CUGAAGUGUUUGGGGGAACUC	1
106	eun-miR167c-3p	GAUCAUGUGGCUGCUUCACC	1
107	eun-miR482a-5p	CAUGGGUCGUUUGGUGAGA	1
108	fve-miR1511	CUAGCUCUGAUACCAUGU	1
109	fve-miR156e	UUGACAGAAGAGAGUGAGCAC	2
110	fve-miR159b	AUUGGAUUGAAGGGAGCUCU	1

No.	Name	Sequence	Reads Count
111	fve-miR162-3p	UCGAUAAAACUCUGCAUCCAG	1
112	fve-miR2109	GUGCAGUGUCUUACUCUG	1
113	fve-miR530	UGCAUUUGCACCUGCACCU	1
114	gma-miR399k	UGCCAAAGGAGAUUUGCCCUG	1
115	gma-miR4994-3p	GACAUCCUUGAGUAAACA	2
116	gma-miR5772	AGAAGUCAGUUAGAGGAG	1
117	lja-miR166-3p	CUUCGGACCAGGCUUCAUUCC	1
118	mtr-miR5247	CAGGAGCAAAGCAUCUGA	1
119	mtr-miR5740	GAAAGAAGAACAUUUGGA	1
120	pab-miR11569	UGCUCUAUGUCAUGGAUC	1
121	pab-miR162a	UCGAUAAACCUCUGCAUCCGG	2
122	pab-miR164a	CACGUGCUCCCCUUCUCC	1
123	pab-miR858b	UUCGUUGUCUGUUCGACCUUG	1
124	peu-miR2916	GGGGCUCGAAGUCGAUCA	1
125	sly-miR159b	UUGGAAAGAGGUGCUCUA	1
126	tae-miR9773	UUUGUUUUUAUGUUAUUU	1
127	vca-miR10202b-5p	AAUAAUCUGUUGGUUCAAACC	2

[a] Filtered clean read from 18 nt to 36 nt in length and perform deduplication to obtain unique reads for subsequent analysis. The obtained unique reads were identified against known plant mature miRNAs in the miRBase22 database (http://www.mirbase.org/)[5] using the criterion of a maximum of two mismatches. Sequences that are not annotated with any information use mireap (v2.0) for new miRNA prediction analysis.

Table S8. MiRNAs that were predicted to target human genes related inflammatory factors[a]

MiRNA	Sequence	Length (nt)	Predicted target gene
han-miR3630-5p	GCAAGUGAUGAAGAACCA	18	TLR4, MyD88, NFKB1, CHUK, claudin1, TJP1(ZO-1), IL-17RA, IL6R, IFN-γ, IL-18, TNFAIP8, TNFAIP8L1
sly-miR168a-3p	CCUGCCUUGCAUCAACUGAAU	21	TLR4, TJP1(ZO-1), IL17A, IL6R, TNFAIP8, TNFAIP2, TNFAIP1
gso-miR1510a	UGUUGUUUUACCUAUUCCACC	21	TLR4, CHUK, IRAK3, IRAK4
mes-miR156k	UUGACAGAAGAGAGAGAGCAC	21	TLR4, IL17RA, IL-1β, IRAK3
bra-miR158-3p	UUUCCAAAUGUAGACAAAGCA	21	TLR4, TJP1 (ZO-1), claudin1, IL6R, TNFAIP8, TNFAIP6, IRAK3
gma-miR482d-3p	UCUUCCCUACACCUCCCAUACC	22	TLR4, claudin 1, IL6R, IL17RA, TNFAIP8, TNFAIP3, IRAK4
aof-miR159	UUUGGAUUGAAGGGAGCUCU	20	TLR4, MyD88, CHUK, claudin 1, TNFAIP8L3, IRAK2
aof-miR167b	UGAAGCUGCCAGCAUGAUCUGA	22	MyD88, IKBKB, IL6R, TNFAIP8, IFNGR2, IRAK3

Table S8. MiRNAs that were predicted to target human genes related inflammatory factors[a] (Continued)

MiRNA	Sequence	Length (nt)	Predicted target gene
aof-miR167c	UGAAGCUGCCAGCAUGAUCU	20	MyD88, IKBKB, occludin, TNFAIP8, IRAK3
aof-miR390	AAGCUCAGGAGGGAUAGCGCC	21	TLR4, occludin, IL17RA, IL6R, TNFAIP8L3
aof-miR394	UUGGCAUUCUGUCCACCUCC	20	TLR4, IL6R, IL17RA, TNFAIP8, TNFAIP1, TNFAIP3
aof-miR166a	UCUCGGACCAGGCUUCAUUCC	21	IL-6R
aof-miR396b	UUCCACAGCUUUCUUGAACUG	21	TLR4, CHUK, TJP1(ZO-1), IL6R, TNFAIP8, TNFAIP8L1, TNFAIP1
eun-miR482a-3p	UCUUGCCAAUACCACCCAUGCC	22	TLR4, IL6R, IL17RA, TNFAIP8, TNFAIP3
ppt-miR894	UUCACGUCGGGUUCACCA	18	TLR4, IL6R
gma-miR1510b-5p	AGGGAUAGGUAAAACAACU	19	TLR4, IL17RA, IL6ST

[a] Sequence information on human mRNAs was collected from the ensembl database (http://asia.ensembl.org/Homo_sapiens/Info/Index;). Miranda (v3.3a) was used in predicting potential human target genes of miRNAs of GENs sample.

TLR4: toll like receptor 4; MyD88: myeloid differentiation primary response gene 88; NFKB1:nuclear factor kappa B subunit 1; CHUK: component of inhibitor of nuclear factor kappa B kinase complex; IKBKB: inhibitor of nuclear factor kappa B kinase subunit beta; TJP1(ZO-1): tight junction protein 1; IL-6R: interleukin 6 receptor; IL6ST: interleukin 6 signal transducer; IL-1β: interleukin 1 beta; IL-17RA: interleukin 17 receptor A; IRAK3/4: interleukin 1 receptor associated kinase 3/4; TNFAIP1/2/3/6/8: TNF alpha induced protein 1/2/3/6/8TNFAIP8L1: TNF alpha induced protein 8 like 1; TNFAIP8L1/3: TNF alpha induced protein 8 like 1/3; IFNGR2: interferon gamma receptor 2; IFN-γ: interferon gamma

Table S9. The sequences of han-miR3630-5p mimic, negative control mimic, wild type (WT) and mutant (MUT) of 3′ UTR fragment of TLR4

Name	Base sequences
han-miR-3630-5p mimic	GCAAGUGAUGAAGAACCA
	UGGUUCUUCAUCACUUGC
negative control mimic	UCACAACCUCCUAGAAAGAGUAGA
	UCUACUCUUUCUAGGAGGUUGUGA
TLR4-WT	GAGCTCCTTTGAGGCTCAGGTCTTAATTCATGAAA T
	GGAGGTAATAATACCTTGTTGGCAGACCTCACTTG G
	TTAAAATGATAATGTTGATAGTTACAATAGTTACA TT
	TAATTGATCAATTGTTTTATGCTCGAG
TLR4-MUT	GAGCTCCTTTGAGGCTCAGGTCTTAATTCATGAAA T
	GGAGGTAATAATACAGGTTTGGCAGAACGACAGG T
	GTTAAAATGATAATGTTGATAGTTACAATAGTTAC AT
	TTAATTGATCAATTGTTTTATGCTCGAG

Blue: putative han-miR-3630-5p binding sites in TLR4 3'UTR

Yellow: mutant han-miR-3630-5p binding sites inTLR4 3'UTR

148 **Reference**

[1] P. Palumbo, U. Picchini, B. Beck, J. van Gelder, N. Delbar and A. DeGaetano, A general approach to the apparent permeability index, *J. Pharmacokinet. Pharmacodyn.*, 2008, **35**, 235–248.

[2] H. S. Cooper, S. N. Murthy, R. S. Shah and D. J. Sedergran, Clinicopathologic study of dextran sulfate sodium experimental murine colitis, *Lab Invest.*, 1993, **69**, 238–249.

[3] F. Shen, J. Feng, X. Wang, Z. Qi, X. Shi, Y. An, Q. Zhang, C. Wang, M. Liu, B. Liu and L. Yu, Vinegar treatment prevents the development of murine experimental colitis via inhibition of inflammation and apoptosis, *J. Agric. Food Chem.*, 2016, **64**, 1111–1121.

[4] a) C. Cao, B. Zhu, Z. Liu, X. Wang, C. Ai, G. Gong, M. Hu, L. Huang and S. Song, An arabinogalactan from Lycium barbarum attenuates DSS-induced chronic colitis in C57BL/6J mice associated with the modulation of intestinal barrier function and gut microbiota, *Food Funct.* 2021, **12**, 9829–9843. b) H. Hao, X. Zhang, L. Tong, Q. Liu, X. Liang, Y. Bu, P. Gong, T. Liu, L. Zhang, Y. Xia, L. Ai and H. Yi, Effect of extracellular vesicles derived from Lactobacillus plantarum Q7 on gut microbiota and ulcerative colitis in mice, *Front Immunol.* 2021, **12**, 777147. c) G. Huang, Z. Wang, G. Wu, R. Zhang, L. Dong, F. Huang, M. Zhang and D. Su, Lychee (Litchi chinensis Sonn.) pulp phenolics activate the short-chain fatty acid-free fatty acid receptor anti-inflammatory pathway by regulating microbiota and mitigate intestinal barrier damage in dextran sulfate sodium-induced colitis in mice, *J. Agric. Food Chem.*, 2021, **69**, 3326–3339.

[5] S. Griffiths-Jones, The microRNA Registry, *Nucleic Acids Res.*, 2004, **32**, D109–111.